This article has been accepted for publication in IEEE Transactions on Power Systems. This is the author's version which has not been fully edited and content may change prior to final publication. Citation information: DOI 10.1109/TPWRS.2022.3196608

Employing Interacting Qubits for Distributed Microgrid Control

Pouya Babahajiani, *Senior Member, IEEE,* Peng Zhang, *Senior Member, IEEE,* Tzu-Chieh Wei, Ji Liu, *Member, IEEE,* Xiaonan Lu, *Member, IEEE*

***Abstract*—To empower flexible and scalable operations, distributed control of multi-inverter microgrids, based on classical communication networks among distributed energy resources, has attracted considerable attention as it can guarantee synchronization and provide suitable remedies to the problem of improper power sharing. Notwithstanding this, resilience of the current schemes on classical communication makes microgrids vulnerable to cyber attacks. Inspired by recent revolutionary breakthroughs in quantum communication, in this paper, we devise a novel synchronization mechanism. We extend the synchronization framework utilized in distributed control algorithms to networks of quantum systems by generating pinning terms and coupling mechanism for the new synchronization rule via exploiting proper quantum jump operators and observables, and show that the quantum system will converge to a time-variant target state. Our devised quantum distributed controller (QDC) gives rise to a novel quantum communication scheme for distributed control of microgrids and enables microgrids to exploit the state-of-the-art quantum communication frameworks as communication infrastructure.**

Test results on two representative AC and DC networked microgrids validate the efficacy and universality of the quantum distributed control.

***Index Terms*—Quantum distributed control, distributed frequency regulation, distributed voltage regulation.**

I. Introduction

MICROGRIDS, featured by the autonomic coordination of their local energy sources and power demands, have proven to be a promising new paradigm of electricity resiliency [1], [2], and thus their share in the energy sector is swiftly growing [3]. In an AC microgrid, distributed energy resources (DERs) provide electrical power that oscillates as sinusoidal waves. Since these waves are finally superimposed, they need to be synchronized to the same (rated) frequency; otherwise, desynchronization of DERs cause the delivered power to fluctuate, which can lead to equipment malfunction and damages and even power outages [4], [5]. Adding to the challenge is the increase in penetrations resulting from the ongoing integration of energy from DERs that are inherently heterogeneous [6], [7] and may further impair the synchronization. Therefore, maintaining frequency synchronization is challenging since the system is complicated in various ways.

Distributed control of multi-inverter microgrids has attracted considerable attention as it can achieve the combined goals of flexible plug-and-play architecture, guaranteeing frequency and voltage regulation while preserving precise power sharing among nonidentical DERs [8]. In distributed control of microgrids, a sparse communication network can be used which has less computational complexity at each inverter controller. As a result, the infrastructure cost can be reduced and the system scalability can be improved. Furthermore, it provides solutions to problems of single point-of-failure and complicated two-way communication networks of central control schemes, offering more reliability while being resilient to faults or unknown system parameters [8], [9].

However, security of communication among distant parties is an indispensable criterion for evaluating the performance of any communication network [10] and distributed control of microgrids is not an exception. While distributed control strategies can enhance microgrids resilience, the openness brought by the corresponding communication networks may cause cybersecurity challenges since they can be susceptible to cyber attacks on communication links. Adversarial attacks from third party agents can drive the microgrid toward inconsistent performance and impair the operation and control functions of participating DERs and stability of the whole system [11].

Finding solutions to encounter cyber manipulation in microgrids with distributed control strategies is an ongoing research [12]–[17]. However, the existing solutions may become insecure due to the rapid development of supercomputers and the emergence of quantum computers [18]–[20] and so they can make traditional/classical methods obsolete. On the other hand, utilizing principles of quantum mechanics, quantum communication offers provable security of communication and is a promising solution to counter such threats [20].

Quantum physics principles give rise to novel capability unattainable with classical transmission media [10], [21]–[24], [24]–[28]. Such a quantum communication enables secure communication between any two points and will connect quantum processors in order to achieve capabilities that are provably impossible by using only classical information [29]. Several major applications have already been reported, including secure communication, quantum distributed computation, simulation of quantum many-body systems and exponential savings in communication [10], [25]. However, central to all these applications is the ability to transmit quantum bits (qubits) which cannot be copied, and any attempt to do so can be detected. This feature makes qubits well suited for security applications [10]. Promising findings on quantum internet have even led some researchers to believe that all secure communications will

This material is based upon work supported in part by the U.S. Department of Energy's Office of Electricity under the Advanced Grid Modeling Program Award No. 37533, in part by the U.S. National Science Foundation under Grant Nos. ECCS-2018492, OIA-2134840 and OIA-2040599, and in part by Stony Brook University's Office of the Vice President for Research through a Quantum Information Science and Technology Seed Grant. T.-C. Wei was supported by the U.S. National Science Foundation under Grant No. PHY-1915165. The views expressed herein do not necessarily represent the views of the National Science Foundation, the U.S. Department of Energy or the United States Government. *(Corresponding author: Peng Zhang.)*

P. Babahajiani, P. Zhang and J. Liu are with the Department of Electrical and Computer Engineering, Stony Brook University, NY 11794, USA (e-mails: pouya.babahajiani, p.zhang, ji.liu @stonybrook.edu).

T. C. Wei is with C.N. Yang Institute for Theoretical Physics, Stony Brook University, NY 11794-3800, USA (e-mail: tzu-chieh.wei@stonybrook.edu).

Xiaonan Lu is with the School of Engineering Technology, Purdue University, West Lafayette, IN, USA (email: xiaonanlu@purdue.edu).

eventually be done through quantum channels [27].

Regarding this revolutionary step in secure communication, many models including quantum key distribution (QKD) [30], quantum teleportation [31] and quantum secure direct communication [32]–[34] have been developed. Based on QKD technology, many different types of quantum communication networks have been proposed [35]–[37]. However, these communication networks based on QKD technology only transmit the key, but do not directly transmit information. On the other hand, quantum secure direct communication is a kind of information carrier with quantum state in communication. In this method, secret information is directly transmitted over a secure quantum channel and, in contrast to QKD schemes, they do not require key distribution and key storage [32].

In this effort, we answer the questions that how is it possible to establish synchronization through exchanging qubits? How can we exploit a quantum communication infrastructure for distributed control of microgrids while control objectives like frequency/voltage regulation and power/current sharing in AC and DC microgrids are guaranteed? Therefore, inspired by the aforementioned developments, specifically those with quantum states in communication, we aim to devise a scalable quantum distributed controller (QDC) for AC and DC microgrids within which, the information carrier is quantum states and the transmission media is a quantum channel, i.e., information is encoded into quantum states which are directly sent over quantum channels among participating DERs. Quantum states are then processed and measured at each DER and the measurement outcomes are exploited as control signals.

One of the primary objectives in distributed control and coordination is to drive a network to reach a consensus, where all agents hold the same value for some key parameter(s), by local interactions [38], [39]. Several efforts have been made to investigate consensus problems in the quantum domain [40]–[42]. To describe quantum state evolution of quantum systems with external inputs (open quantum systems), a so called Lindblad equation can be used [43], [44]. Authors in [45] show that quantum consensus can be obtained through a Lindblad master equation with the Lindblad terms generated by swapping operators among the qubits, giving rise to the dynamical evolution of the quantum network. The swapping operations also introduce an underlying interaction graph for the quantum network, which leads to a distributed structure for the master equation.

One existing approach to achieve quantum consensus is to model the quantum network's state evolution through the quantum synchronization master equation [45]. Another approach is to appeal to the gossip-type interaction between neighboring quantum computing devices [41]. Existing literature only considers two special cases: 1) Under a non-zero Hamiltonian with the swapping as jump operators, each qubit tends to the same trajectory corresponding to a network Hamiltonian and initial states; 2) Under a zero Hamiltonian, the network's final state is the average of the initial states. In both cases, however, it is difficult to derive the explicit trajectory of each qubit as a function of the Hamiltonian, and the synchronization orbit is certainly no longer the one determined by the Hamiltonian for most choices of the Hamiltonian [45]. Furthermore, in the existing approaches, measurement is not considered, i.e., the existing frameworks are valid as long as the corresponding quantum system is not measured, which makes them impractical for realistic distributed control of microgrids.

Toward the goal of devising the quantum distributed controller, considering the above challenges and potential to design a quantum synchronization scheme, we first formulate the quantum synchronization problem using a quantum master equation and identify and characterize suitable jump operators to drive the quantum network to synchronization. The protocol we construct gives rise to a differential equation that allows us to analyze the convergence. We utilize proper observables and show that all the corresponding expectation values (averaging measurement outcomes) will eventually converge to a possibly time-varying target value, and finally exploit these expectation values to construct the control signals to drive a network of DERs to synchronization.

Hence, our devised QDC gives rise to a novel quantum communication scheme for distributed control of microgrids and enables microgrids to utilize the existing quantum communication frameworks as communication infrastructure, and also paves the way for more advanced quantum-secure communication frameworks for microgrids, unattainable with classical transmission media.

The rest of the paper is organized as follows. Section II provides some preliminaries including relevant concepts in graph theory and quantum systems along with notations and conventions we use in this paper. The developed quantum distributed controller together with a numerical example and proof of convergence are presented in section III. Section IV is devoted to explain the devised quantum distributed frequency controller and voltage controller for AC and DC microgrids, respectively. Simulation results are also provided. Section V provides a discussion on realization of QDC, summarizes the main results and gives an outlook on possible further developments and applications.

II. Preliminaries

In this section, we introduce some fundamental concepts from graph theory [46] and quantum systems [47].

A. Graph Theory

Some basic concepts from graph theory [46] are provided here. A simple graph $G = (V, E)$ consists of a set of n nodes (or agents), $V = \{v_1, v_2, \ldots, v_n\}$, and a set of edges, $E \subset V \times V$. An edge $(v_i, v_j) \subset E$ represents that agents v_i and v_j can exchange information with each other. A sequence of non-repeated edges $(v_i, v_{p_1}), (v_{p_1}, v_{p_2}), \ldots, (v_{p_{m-1}}, v_{p_m}), (v_{p_m}, v_j)$ is called a path between nodes v_i and v_j. If there exists a path between any two different nodes $v_i, v_j \in V$, G is said to be connected. An agent v_j is called a neighbor of agent v_i if $(v_j, v_i) \subset E$. The set of neighbors of agent v_i is denoted as $N_i = \{v_j \in V \mid (v_j, v_i) \subset E\}$. The adjacency matrix of graph G, denoted as A, is an $n \times n$ matrix whose entries $a_{i,j} = 1$ if $v_j \in N_i$ and $a_{i,j} = 0$ otherwise. The degree matrix D of graph G, denoted as D, is defined as an $n \times n$ diagonal matrix whose ith diagonal entry equals the degree of node v_i, i.e., $\sum_{v_j \in N_i} a_{i,j}$. The Laplacian matrix of graph G, denoted as L, is defined as $D - A$. Note that A, D, L are all symmetric. The

This article has been accepted for publication in IEEE Transactions on Power Systems. This is the author's version which has not been fully edited and content may change prior to final publication. Citation information: DOI 10.1109/TPWRS.2022.3196608

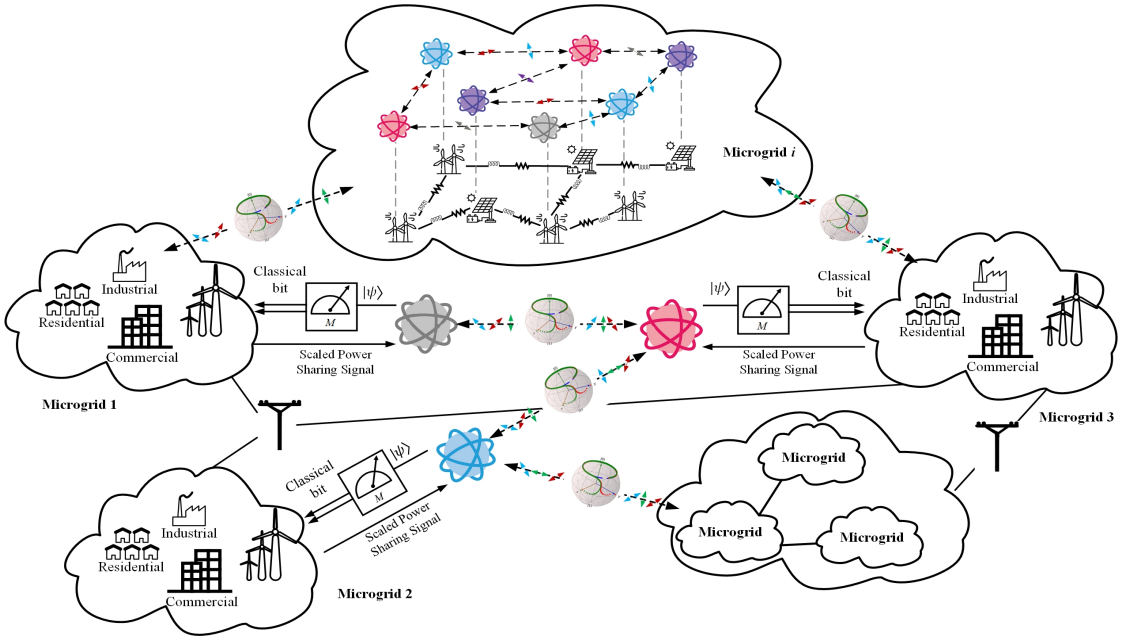

Fig. 1. QDC framework for microgrids - Quantum communication is established among the DERs - Power sharing signals, n_iP_i, are scaled to be encoded into quantum information.

node-edge incidence matrix $B \in R^{V\times E}$ is defined component-wise as $B_{i,j} = 1$ if edge j enters node i, $B_{i,j} = -1$ if edge j leaves node i, and $B_{i,j} = 0$ otherwise. For $x \in R^V$, $B^T x \in R^E$ is the vector with components $x_i - x_j$, with $\{i, j\} \in E$. If $\text{diag}(\{a_{i,j}\}_{\{i,j\}\in E})$ is the diagonal matrix of edge weights, then the Laplacian matrix is given by $L = B\,\text{diag}(\{a_{i,j}\}_{\{i,j\}\in E})B^T$.

B. Quantum Systems and Notations

Throughout this paper, the (adjoint) $\dagger$ symbol indicates the transpose-conjugate in matrix representation, and the tensor product symbol $\otimes$ is the Kronecker product.

The mathematical description of a single quantum system starts by considering a complex Hilbert space $\mathcal{H}$. We utilize Dirac's notation, where $|\psi\rangle$ denotes an element of $\mathcal{H}$, called a ket which is represented by a column vector, while $\langle\psi| = |\psi\rangle^\dagger$ is used for its dual, a bra, represented by a row vector, and $\langle\psi|\varphi\rangle$ for the associated inner product. We denote the set of linear operators on $\mathcal{H}$ by $\mathfrak{B}(\mathcal{H})$. The adjoint operator $X^\dagger \in \mathfrak{B}(\mathcal{H})$ of an operator $X \in \mathfrak{B}(\mathcal{H})$ is the unique operator that satisfies $(X|\psi\rangle)^\dagger |\chi\rangle = \langle\psi| (X^\dagger |\chi\rangle)$ for all $|\psi\rangle, |\chi\rangle \in \mathcal{H}$. The natural inner product in $\mathfrak{B}(\mathcal{H})$ is the Hilbert-Schmidt product $\langle X, Y\rangle = \text{tr}(X^\dagger Y)$, where tr is the usual trace functional which is canonically defined in a finite dimensional setting. We denote by I the identity operator. $[A, B] = AB - BA$ is the commutator and $\{A, B\} = AB + BA$ is the anticommutator of A and B.

A quantum bit (qubit), defined as the quantum state of a two-state quantum system, is the smallest unit of information, and it is analogous to a classical bit. The state of a qubit, represented by $|\psi\rangle = \alpha|0\rangle + \beta|1\rangle$, is a superposition of the two orthogonal basis states $|0\rangle$ and $|1\rangle$, where α and β are complex numbers in general, where $|\alpha|^2 + |\beta|^2 = 1$. We will simplify the notation of a n-qubit state $|q_1\rangle \otimes ... \otimes |q_n\rangle \in \mathcal{H}^{\otimes n}$ as $|q_1...q_n\rangle$.

In the case of mixed state, the state of a quantum system is represented by a *density operator* ρ, which is a self-adjoint positive semi-definite operator with trace one. Moreover, the state $|\psi\rangle \in \mathcal{H}$ with $\langle\psi|\psi\rangle = 1$ in the above is called a pure state, which can also be written in the form of a density matrix $\rho = |\psi\rangle\langle\psi|$. For further information on qubits see [47], [48].

III. Quantum Distributed Control

Distributed control problems of microgrids are typically modeled as networked differential equations over a simple, connected graph $G = (V, E)$ whose node set $V = \{v_1, v_2, \ldots, v_n\}$ represents microgrids and edge set E depicts allowable communication among the microgrids. As an illustrative example, the problem of distributed frequency control and power sharing in AC microgrids can be formulated as

$$\begin{aligned} \omega_i &= \omega^* - n_iP_i + \Phi_i, \\ \dot{\Phi}_i &= f(\Phi_i,\ P_i,\ \Phi_j,\ j \in N_i), \end{aligned} \tag{1}$$

where ω_i represents the derivative of the voltage phase angle of DER$_i$ (i.e., the frequency at DER$_i$) with respect to time, ω^* is a nominal network frequency, P_i is the measured active power injection at DER$_i$, n_i is the gain of the droop coefficient, N_i denotes the set of neighbors of DER$_i$ (i.e., $N_i = \{v_j \in V \mid (v_j, v_i) \subset E\}$), and the dynamics of Φ_i represents the secondary control, which is a function (f) of its current value, P_i, and Φ_j's of its neighbors. The goal of the distributed frequency control problem is to ensure that the network frequency will be regulated to the rated value ω^* and that active power sharing is guaranteed (i.e., $\omega_i = \omega^*$ and $n_iP_i = n_jP_j$ for all i, j). It is worth emphasizing that Eq. (1) has a universal form which can be used, with simple modification, to describe the problem of distributed voltage control and power/current sharing in DC microgrids, as we will elaborate in section IV.

Recent development in quantum algorithms for solving linear/nonlinear/partial differential equations suggests potential efficiency and capability of quantum devices in solving these class of equations [49]–[55]. Therefore, we aim to construct a

This article has been accepted for publication in IEEE Transactions on Power Systems. This is the author's version which has not been fully edited and content may change prior to final publication. Citation information: DOI 10.1109/TPWRS.2022.3196608

quantum distributed framework to control a network of DERs, as shown in Fig. 1. In this framework, each DER is equipped with or connected to a quantum computing (QC) device, which prepares a quantum state to be manipulated and measured and then seeks a consensus among all the QCs in a distributed manner.

The state of each quantum device can be described by a positive Hermitian density matrix ρ. Since synchronization requires interaction among all quantum devices, let us assume that each device can be considered as a quantum system and has access to the (quantum) information of its neighbors. The following Lindblad master equation is a suitable way to describe the dynamics of a system with dissipation:

$$\dot{\rho}(t) = -\frac{\imath}{\hbar}[H,\rho] + \sum_{i=1}^{n}\Big(C_i\rho C_i^\dagger - \frac{1}{2}\{C_i^\dagger C_i,\rho\}\Big), \tag{2}$$

where H is the effective Hamiltonian as a Hermitian operator over the underlying Hilbert space, $\hbar$ is the reduced Planck constant, $\imath$ denotes the imaginary unit (i.e., $\imath^2 = -1$), and C_i's are jump operators. For more information on Markovian master equations in Lindblad form, see [56]. To anticipate later discussions, it should be emphasized that our goal is to leverage the Lindblad master equation in order to construct the network of differential equations, such as those in Eq. (1), in which, in contrast to the classical synchronization, quantum bits are what is exchanged among the nodes. We next demonstrate that utilizing suitable jump operators and observers for each quantum node would lead the average expectation values of all the observers in the corresponding quantum setting to converge to a possibly time-varying target value and the synchronization rule follows the Kuramoto model modified by the presence of a sinusoidal driving [57].

A. Algorithm

Let us update the state of each quantum node at each time step as follows:

$$|q_i(t)\rangle = \begin{pmatrix}\cos\frac{\pi}{4}\\ e^{\imath\phi_i(t)}\sin\frac{\pi}{4}\end{pmatrix}, \qquad t\in\{0,1,2,\ldots\}, \tag{3}$$

which is the general state in polar coordinates set on the xy-plane in the Bloch sphere, where $\phi_i(0)\in(0,\pi/2)$ and each $\phi_i(t)$, $t\geq 1$, is the averaged measurement outcome which can be obtained by simply averaging measurement outcomes of many realizations of a single experiment for node i and will be discussed in detail shortly. Let $|\psi\rangle = |q_1 q_2\cdots q_n\rangle$ be the state of the whole quantum network and $\rho = |\psi\rangle\langle\psi|$. We introduce the following master equation:

$$\begin{aligned}\dot{\rho}(t) = &\sum_{i=1}^{n}\Big(C_i\rho C_i^\dagger - \frac{1}{2}\{C_i^\dagger C_i,\rho\}\Big)\\ &+\sum_{\{i,j\}\in E}\Big(C_{i,j}\rho C_{i,j}^\dagger - \frac{1}{2}\{C_{i,j}^\dagger C_{i,j},\rho\}\Big).\end{aligned} \tag{4}$$

where $C_{i,j}$ is the swapping operator that specifies the external interaction between quantum computing devices i and j such that

$$\begin{aligned}&C_{i,j}(|q_1\rangle\otimes\ldots\otimes|q_i\rangle\otimes\ldots\otimes|q_j\rangle\otimes\ldots\otimes|q_n\rangle)\\ &\qquad = |q_1\rangle\otimes\ldots\otimes|q_j\rangle\otimes\ldots\otimes|q_i\rangle\otimes\ldots\otimes|q_n\rangle\,.\end{aligned} \tag{5}$$

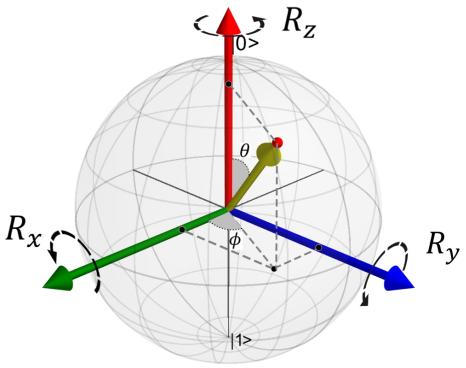

Fig. 2. Qubit state representation on the Bloch sphere. Rotations around the positive X, Y, and Z axes are represented by the dashed black arrows.

Let us define the jump operator, C_i, by

$$C_i = I^{\otimes(i-1)}\otimes R_z(\phi)\otimes I^{\otimes(n-i)} \tag{6}$$

with $R_z(\phi)$ being the rotation-Z operator which is a single-qubit rotation through angle ϕ radians around the Z-axis (Fig. 2):

$$R_z(\phi) = \begin{pmatrix}e^{-\imath\phi/2} & 0\\ 0 & e^{\imath\phi/2}\end{pmatrix}. \tag{7}$$

By definition, the operator C_i acts only on $|q_i\rangle$ without changing the states of other qubits, i.e.,

$$\begin{aligned}C_i\rho C_i^\dagger &= C_i\left(\left|\overbrace{q_1\ \ldots}^{\text{i-1}}\,q_i\,\overbrace{\ldots\ q_n}^{\text{n-i}}\right\rangle\left\langle\overbrace{q_1\ \ldots}^{\text{i-1}}\,q_i\,\overbrace{\ldots\ q_n}^{\text{n-i}}\right|\right)C_i^\dagger\\ &= \left|\overbrace{q_1\ \ldots}^{\text{i-1}}\,q_i'\,\overbrace{\ldots\ q_n}^{\text{n-i}}\right\rangle\left\langle\overbrace{q_1\ \ldots}^{\text{i-1}}\,q_i'\,\overbrace{\ldots\ q_n}^{\text{n-i}}\right|\end{aligned} \tag{8}$$

To see the impact of the introduced jump operator on $|q_i\rangle$, by selecting $\phi = \phi_{t,i} - \phi_i$ we have

$$\begin{aligned}&R_z(\phi)\,|q_i\rangle\,\langle q_i|\,R_z^\dagger(\phi) =\\ &\qquad\begin{pmatrix}\cos^2\frac{\pi}{4} & e^{-\imath(\phi_i+\phi)}\cos\frac{\pi}{4}\sin\frac{\pi}{4}\\ e^{\imath(\phi_i+\phi)}\cos\frac{\pi}{4}\sin\frac{\pi}{4} & \sin^2\frac{\pi}{4}\end{pmatrix}\\ &\qquad = \begin{pmatrix}\cos\frac{\pi}{4}\\ e^{\imath(\phi_{t,i})}\sin\frac{\pi}{4}\end{pmatrix}\begin{pmatrix}\cos\frac{\pi}{4} & e^{-\imath(\phi_{t,i})}\sin\frac{\pi}{4}\end{pmatrix}\end{aligned} \tag{9}$$

which is considered as the target state for quantum node i. As can be seen, the jump operators C_i's are state dependent and updated based on the target values $\phi_{i,t}$ and the measured $\phi_i(t)$. Furthermore, as mentioned, at the beginning of each time step, all the qubits are initialized as (3) based on the measurement outcome of the previous step. Therefore, at each time step, the master equation components are updated based on the target values and the obtained measurement signals. Thus, the density matrix at time $t+dt$ can be decomposed into $\rho(t+dt) = \rho(t) + d\rho_t$, where $d\rho(t)$ is defined in (4).

In order to obtain the angles ϕ_i, we introduce the following observables:

$$A_{1,i} = I^{\otimes(i-1)}\otimes\sigma_x\otimes I^{\otimes(n-i)}, \tag{10}$$

$$A_{2,i} = I^{\otimes(i-1)}\otimes\sigma_y\otimes I^{\otimes(n-i)}. \tag{11}$$

This article has been accepted for publication in IEEE Transactions on Power Systems. This is the author's version which has not been fully edited and content may change prior to final publication. Citation information: DOI 10.1109/TPWRS.2022.3196608

The operator $I^{\otimes(i-1)} \otimes \sigma_{x/y} \otimes I^{\otimes(n-i)}$ acts only on $|q_i\rangle$ where node-wise means, having σ_x and σ_y which are Pauli matrices as observables at each node,

$$\sigma_x = \begin{pmatrix} 0 & 1 \\ 1 & 0 \end{pmatrix}, \qquad \sigma_y = \begin{pmatrix} 0 & -\imath \\ \imath & 0 \end{pmatrix}. \tag{12}$$

The expectation value of an observable A via measurement on a system described a density matrix ρ is given by $\langle A \rangle = \mathrm{tr}(\rho \mathrm{A})$ [48]. For a general one qubit state ρ, $\mathrm{tr}(\rho\sigma_x) = r\sin\theta\cos\phi$, $\mathrm{tr}(\rho\sigma_y) = r\sin\theta\sin\phi$ and $\mathrm{tr}(\rho\sigma_z) = r\cos\theta$, where r, θ, and ϕ are the parameters that describe ρ in the Bloch sphere, which is essentially the spherical coordinate but with $r \leq 1$. Generally, the Lindblad equation results in states becoming more mixed; however, we only let the system evolve in a short time and re-initialize the system in a product of pure qubit states. Therefore, we can consider $r = 1$ and $\theta = \pi/2$ and hence

$$\mathrm{tr}(\rho\sigma_{\mathrm{x}}) = \cos\phi_{\mathrm{i}}, \qquad \mathrm{tr}(\rho\sigma_{\mathrm{y}}) = \sin\phi_{\mathrm{i}}. \tag{13}$$

which are equivalent to $\mathrm{tr}(\rho \mathrm{A}_{1,\mathrm{i}}) = \cos\phi_{\mathrm{i}}$ and $\mathrm{tr}(\rho \mathrm{A}_{2,\mathrm{i}}) = \sin\phi_{\mathrm{i}}$, respectively. Since both C_i and $C_{i,j}$ are unitary, we have

$$d\rho(t) = \sum_{i=1}^{n}(C_i\rho C_i^\dagger - \rho)dt + \sum_{\{i,j\}\in E}(C_{i,j}\rho C_{i,j}^\dagger - \rho)dt, \tag{14}$$

If we repeat the procedure of the Lindblad evolution in a short duration, measurement and re-initialization, we can obtain approximated equations for ϕ_i's in the limit $dt \to 0$. The goal is to obtain the dynamic of the phase angles ϕ_i. Note that $\frac{d}{dt}\langle A\rangle = \frac{d}{dt}\mathrm{tr}(\rho \mathrm{A}) = \mathrm{tr}(\dot{\rho}\mathrm{A})$. From (14),

$$\begin{aligned} \mathrm{tr}(\dot{\rho}\mathrm{A}_{1,\mathrm{i}}) &= \cos\phi_{t,i} - \cos\phi_i + \sum_{j=1}^{n} a_{i,j}(\cos\phi_j - \cos\phi_i) \\ \mathrm{tr}(\dot{\rho}\mathrm{A}_{2,\mathrm{i}}) &= \sin\phi_{t,i} - \sin\phi_i + \sum_{j=1}^{n} a_{i,j}(\sin\phi_j - \sin\phi_i) \end{aligned} \tag{15}$$

where $a_{i,j} = 1$ if $C_{ij} \neq \mathbf{0}$ and $a_{i,j} = 0$ otherwise. Utilizing $\mathrm{tr}(\rho \mathrm{A}_{1,\mathrm{i}})$ and $\mathrm{tr}(\rho \mathrm{A}_{2,\mathrm{i}})$, we have the dynamic of ϕ_i as follows:

$$\begin{aligned} \dot{\phi}_i &= \frac{d}{dt}\arctan\left(\frac{\mathrm{tr}(\rho \mathrm{A}_{2,\mathrm{i}})}{\mathrm{tr}(\rho \mathrm{A}_{1,\mathrm{i}})}\right) \\ &= \left\{\frac{tr(\dot{\rho}A_{2,i})tr(\rho A_{1,i}) - tr(\dot{\rho}A_{1,i})tr(\rho A_{2,i})}{\cos^2\phi_i}\right\}\cos^2\phi_i \\ &= \left(\sin\phi_{t,i} - \sin\phi_i + \sum_{j=1}^{n} a_{i,j}(\sin\phi_j - \sin\phi_i)\right)\cos\phi_i \\ &- \left(\cos\phi_{t,i} - \cos\phi_i + \sum_{j=1}^{n} a_{i,j}(\cos\phi_j - \cos\phi_i)\right)\sin\phi_i \\ &= \sin(\phi_{t,i} - \phi_i) + \sum_{j=1}^{n} a_{i,j}\sin(\phi_j - \phi_i). \end{aligned} \tag{16}$$

It is worth mentioning that both $\mathrm{tr}(\rho \mathrm{A}_{1,\mathrm{i}})$ and $\mathrm{tr}(\rho \mathrm{A}_{2,\mathrm{i}})$ are used in (16) to find the trajectory that ϕ_i traverses along the time; however, either $\arccos(\mathrm{tr}(\rho\sigma_{\mathrm{x}}))$ or $\arcsin(\mathrm{tr}(\rho\sigma_{\mathrm{y}}))$ gives ϕ_i. In the 'Analysis' subsection, we will show how the pinning term $\sin(\phi_{t,i} - \phi_i)$ forces the phase ϕ_i to stick at the value $\phi_{t,i}$ and the coupling mechanism $\sum_{j=1}^{n} a_{i,j}\sin(\phi_j - \phi_i)$ helps to synchronize the entire system.

The basic outline of the algorithm is drawn schematically in Fig. 3 and is summarized as follows:

1) Initialize qubits as a point on the first quarter of the equator of the Bloch Sphere, i.e., $0 < \phi_i(0) < \pi/2$, using Eq. (3).
2) Teleport information throughout the network such that each quantum node receives the quantum information from its adjacent nodes.
3) At each node, update the rotation-Z (R_z) operator's argument based on the pinner ($\phi_{t,i}$) and the current value of the phase angle ϕ_i.
4) Evolve the master Eq. (14) for one time step δt by means of the swapping and rotation-Z operators.
5) Measure the expectation value of the σ_x or σ_y operator as the observer at each node. Repeating this multiple times and averaging gives the $\cos\phi_i$ or $\sin\phi_i$, depending on the exploited observable.
6) On classical hardware at each node, compute $\arccos\langle\sigma_x\rangle$ or $\arcsin\langle\sigma_y\rangle$ to obtain the phase angle ϕ_i.
7) Re-initialize the state of each quantum node according to Eq. (3).
8) Go back to step 2.

B. Analysis

For synchronization of the system, it is critical that the pinner for all of the oscillators be the same, i.e., $\phi_{t,i} = \phi^*$, otherwise, synchronization cannot be achieved in general. To study whether quantum node i is synchronized to the pinner, it is convenient to study the phase deviation of quantum node i from the pinner. We introduce the following change of variables,

$$\phi_i = \phi^* + \zeta_i, \tag{17}$$

where ζ_i denotes the phase deviation of the ith oscillator from the pinner ϕ^*. Substituting (17) into (16), we have

$$\dot{\zeta}_i = \sum_{j=1}^{n} a_{i,j}\sin(\zeta_j - \zeta_i) - \sin(\zeta_i). \tag{18}$$

By studying the properties of (18), we can obtain the condition for synchronization. If all ζ_i's converge to 0, then we have $\phi_i = \phi^*$ as $t \to \infty$, indicating that all nodes are synchronized to the pinner. Let $B = [B_{i,j}]_{n\times m}$ be the incidence matrix [46] of the communication graph G with m being the number of edges. Then, (18) can be recast in a state form:

$$\dot{\zeta} = -\sin\zeta - BW\sin\big(B^T\zeta\big), \tag{19}$$

where $W = \mathrm{diag}(\{a_{i,j}\}_{\{i,j\}\in E})$ is the diagonal matrix of edge weights and $\sin(\cdot)$ takes entry-wise operation for a vector.

To proceed, set $\varepsilon = \max_{1\leq i\leq n}|\zeta_i|$. When $\varepsilon < (\pi/2)$, if $\zeta_i = \varepsilon$, we have $-\pi < -2\varepsilon \leq \zeta_j - \zeta_i \leq 0$ for $1 \leq j \leq n$. Hence, in (18), $\sin(\zeta_j - \zeta_i) \leq 0$ and $\sin\zeta_i > 0$ hold, and hence $\dot{\zeta}_i < 0$ hold. Therefore, the vector field is pointing inward in the set, and no trajectory can escape to values larger than ε. Similarly, it can be obtained that, when $\zeta_i = -\varepsilon$, $\dot{\zeta}_i > 0$ holds. Thus no trajectory can escape to values smaller than $-\varepsilon$. Therefore, $\zeta \in [-\varepsilon,\varepsilon]\times\cdots\times[-\varepsilon,\varepsilon] = [-\varepsilon,\varepsilon]^n$ is positively invariant

This article has been accepted for publication in IEEE Transactions on Power Systems. This is the author's version which has not been fully edited and content may change prior to final publication. Citation information: DOI 10.1109/TPWRS.2022.3196608

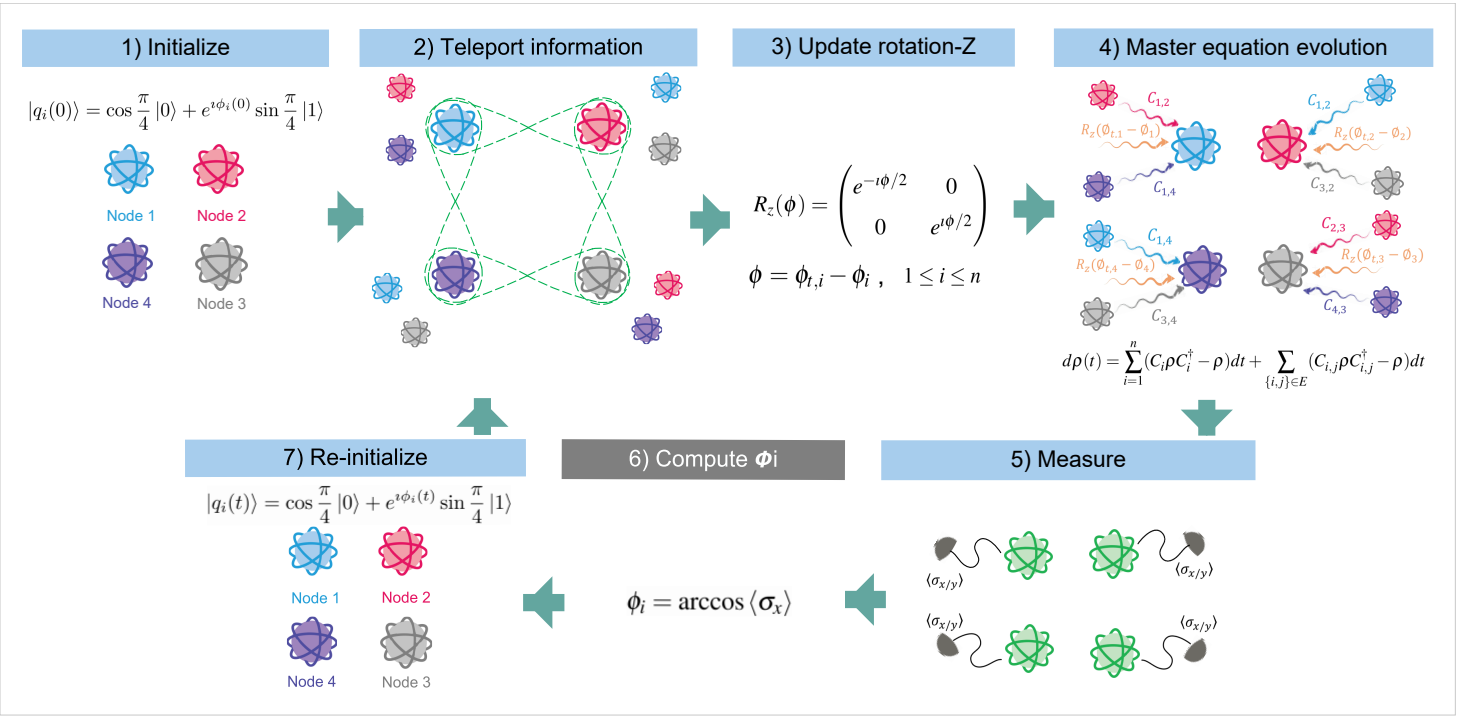

Fig. 3. Schematic depiction of the QDC - At step 1), $\phi_i(0) \in (0, \pi/2)$ - If at step 5) σ_y operator is used as observer to measure the qubit at each node, at step 6), ϕ_i is calculated by $\phi_i = \arcsin\langle\sigma_y\rangle$ - At step 7), the averaged measurement outcome of step 6) is utilized to re-initialize the qubits.

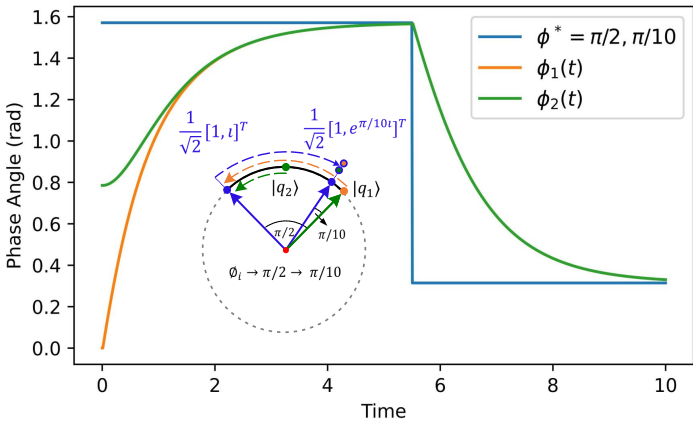

Fig. 4. Quantum state tracking - Exponential synchronization of phase angles - The selected time step for the numerical example is 10^{-4} - The final state is $\frac{1}{\sqrt{2}}[1,\ e^{\pi/10\imath}]^T$.

when $\varepsilon < \pi/2$, where $\times$ denotes Cartesian product. Define a Lyapunov function $V = (1/2)\zeta^T\zeta$, which equals zero only if all ζ_i are zero, meaning the synchronization of all nodes to the pinner. Differentiating V along the trajectories of (19) yields

$$\begin{aligned} \dot{V} = \zeta^T\dot{\zeta} &= -\zeta^T\left(\sin\zeta + BW\sin B^T\zeta\right) \\ &= -\zeta^T S_1\zeta - \zeta^T BWS_2B^T\zeta, \end{aligned} \tag{20}$$

where $S_1 \in R^{n\times n}$ and $S_2 \in R^{m\times m}$ are given by

$$\begin{aligned} S_1 &= \text{diag}\left\{\text{sinc}(\zeta_1), \cdots, \text{sinc}(\zeta_n)\right\}, \\ S_2 &= \text{diag}\left\{\text{sinc}(B^T\zeta)_1, \cdots, \text{sinc}(B^T\zeta)_m\right\}, \end{aligned} \tag{21}$$

where sinc(x) $\equiv$ sin(x)/x and $(B^T\zeta)_i$ denotes the ith element of $m\times 1$ dimensional vector $B^T\zeta$. When all ζ_i are within $[-\varepsilon, \varepsilon]$ with $0 \le \varepsilon < (\pi/2)$, $(B^T\zeta)_i$ is in the form of $\zeta_k - \zeta_l$ $(1 \le k, l \le n)$, and hence is restricted to $(-\pi, \pi)$. Given that in $(-\pi, \pi)$, sinc(x) > 0 holds, it follows that S_1 and S_2 satisfy the following inequalities:

$$\begin{aligned} S_1 &\ge \sigma_1 I, \quad \sigma_1 = \text{sinc}(\varepsilon), \\ S_2 &\ge \sigma_2 I, \quad \sigma_2 = \text{sinc}(2\varepsilon). \end{aligned} \tag{22}$$

So, we have $S_1 + BWS_2B^T \ge \sigma_1 I + \sigma_2 BWB^T$, which in combination with (20) yields

$$\dot{V} \le -\zeta^T(\sigma_1 I + \sigma_2 BWB^T)\zeta. \tag{23}$$

Note that BWB^T is the Laplacian matrix of the underlying graph G, which is always positive semidefinite. Since σ_1 and σ_2 are positive, $\sigma_1 I + \sigma_2 BWB^T$ must be positive definite. It follows that, when $0 \le \varepsilon < (\pi/2)$, we have $\dot{V} \le -2\mu V$, where

$$\mu = \lambda_{\min}(\sigma_1 I + \sigma_2 BWB^T) > 0, \tag{24}$$

which implies that all the nodes will synchronize to the pinner exponentially fast at a rate no less than μ, which is dependent on the network connectivity.

C. Numerical Example

We consider a network composed of two quantum nodes with the following initial states:

$$|q_1\rangle = \frac{1}{\sqrt{2}}\begin{pmatrix}1\\1\end{pmatrix}, \qquad |q_2\rangle = \begin{pmatrix}1/\sqrt{2}\\0.5+0.5\imath\end{pmatrix}.$$

In this example, the state $\frac{1}{\sqrt{2}}[1,\ \imath]^T$ is the first target, then at t = 5.5 the target changes to the state $\frac{1}{\sqrt{2}}[1,\ e^{\pi/10\imath}]^T$ and hence, the pinner is $\phi^* = \pi/2$ and then $\phi^* = \pi/10$, respectively. The two qubits $|q_1\rangle$ and $|q_2\rangle$ interact through a swapping operator, forming a connected interaction graph. The trajectories

This article has been accepted for publication in IEEE Transactions on Power Systems. This is the author's version which has not been fully edited and content may change prior to final publication. Citation information: DOI 10.1109/TPWRS.2022.3196608

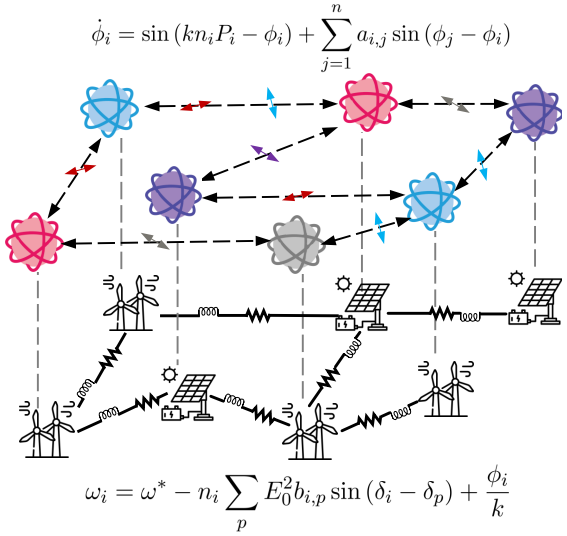

Fig. 5. Coupling of the physical microgrid to the network of quantum controllers can be considered as coupling of Kuramoto models.

of ϕ_1 and ϕ_2, i.e. phase angles of $|q_1\rangle$ and $|q_2\rangle$ respectively, are sketched in Fig. 4 utilizing the Python-based open source software QuTiP [58]. As illustrated, both phase angles converge to ϕ^*. Therefore, the final state of the quantum network is $|qq\rangle$, where we denote by $|q\rangle$ the state $\frac{1}{\sqrt{2}}[1,\ e^{\pi/10\imath}]^T$.

IV. Quantum Distributed Controller for AC and DC Microgrids

A. Quantum Distributed Frequency Control

In AC microgrids, a predominantly inductive network naturally decouples the load sharing process; the reactive power regulator must handle the reactive load sharing by adjusting voltage magnitude while the active power regulator would handle the active load sharing through adjusting the frequency. A common approach for inverter interfaced DER is to connect the power electronic inverter with an LC filter. Therefore, the predominantly inductive line is either from the natural line/cable characteristics or implemented with virtual impedance. The locally deployed LC filter in each DER makes the output impedance inductive dominant [59], then the power sharing control laws that allow the active power to be shared based on DER units' rated capacities according to the droop setting, can be written as [60]

$$\omega_i = \omega^* - n_i P_i \tag{25}$$

As discussed, the problem of distributed frequency control and power sharing would take a form such as Eq. (1) where Φ_i as the secondary controller is a synchronization rule consisting of pinning terms and coupling mechanism and is a function of its current value, P_i, and its neighbors' values Φ_j's. Looking at Eq. (16), it can be seen that there are pinning terms, produced by the rotation-Z operators and coupling mechanism, produced by swapping operators. Therefore, in order to apply the QDC, we need to define the target for (16) which is done through scaling n_iP_i. Here, we call n_iP_i the power sharing signal. Specifically, n_iP_i is scaled to be restricted to in the range $(0, \pi/2)$; thus, we select k such that $k < \frac{\pi/2}{\max(n_iP_i)}$ so that, kn_iP_i is ready to be incorporated into the argument of the rotation-Z operator at node i and then the process follows the steps explained in Fig. 3. Hence, our developed QDC for AC microgrids is formulated as follows

$$\begin{aligned} \omega_i &= \omega^* - n_iP_i + \frac{\phi_i}{k}, \\ \dot{\phi}_i &= \sin(kn_iP_i - \phi_i) + \sum_{j=1}^{n} a_{i,j}\sin(\phi_j - \phi_i), \end{aligned} \tag{26}$$

where ϕ_i/k is the secondary control variable.

In a typical AC microgrid with distributed line impedances, since the susceptance of line impedance is usually much larger than its conductance, and also due to the small angle difference between each bus voltage, the active power and reactive power are decoupled and the output active power of each DER can be expressed as [61]

$$P_i = \sum_{p=1}^{n} E_iE_p|Y_{i,p}|\sin(\delta_i - \delta_p) = \sum_{p=1}^{n} g_{i,p}\sin(\delta_i - \delta_p) \tag{27}$$

where E_i is the nodal voltage magnitudes $E_i > 0$, $-Y_{i,p}$ is the admittance of the line between DER$_i$ and DER$_p$ and δ_i is the voltage phase angle and its dynamic characteristic is $\dot{\delta}_i = \omega_i - \omega^* = \phi_i/k - n_iP_i$.

From (27), the physical power network can be treated as a connected network whose entries of its adjacency matrix are $g_{i,p} = E_iE_p|Y_{i,p}|$ and hence, considering (26), it can be readily obtained that, the coupling of the network of quantum distributed controllers and the physical microgrid is the coupling of a forced Kuramoto model with a Kuramoto model (Fig. 5). At the steady state, the microgrid is assumed stable. Since the DERs' frequency must be equal, we have $\omega_i = \omega_j$ and thus $n_iP_i - \phi_i/k = n_jP_j - \phi_j/k \quad \forall i,j$. As shown before, ϕ_i converges to the pinner as $t \to \infty$. Thus, $n_iP_i = \phi_i/k$ and $n_iP_i = n_jP_j \quad \forall i,j$ and ω_i converges to ω^*.

B. Verification on an AC Networked-Microgrid Case Study

The performance of the developed quantum distributed controller is tested on a networked microgrids with five AC microgrids each one has 3 DERs (Fig. 6). The nominal voltage and frequency are 380 V and 60 Hz respectively. All other parameters can be seen in Fig. 6. For the sake of simulation, two scenarios are examined. In the first scenario, the system is examined in the face of a step load change. To verify the QDC's feature of plug-and-play capability, as the second scenario, plug-and-play of DERs and microgrids are tested.

1) Controller Performance: Studies in this section illustrate the performance of the QDC under a step load change applied to microgrid 2 at t = 10s and results are depicted in Fig. 7. The exploited communication graph is shown in Fig. 6. As can be seen, frequency regulation is maintained throughout the step load change and Active power is accurately shared among the heterogeneous DGs throughout the entire runtime.

2) Plug-and-play functionality - plug-and-play of DERs: Due to the availability of renewable generators, microgrid's physical and communication topologies can be time-varying. In this case we demonstrate that to support plug-and-play functionality, our developed QDC provides a robust secondary control framework that works effectively in spite of time-varying communication networks. Thus, this case verifies the

This article has been accepted for publication in IEEE Transactions on Power Systems. This is the author's version which has not been fully edited and content may change prior to final publication. Citation information: DOI 10.1109/TPWRS.2022.3196608

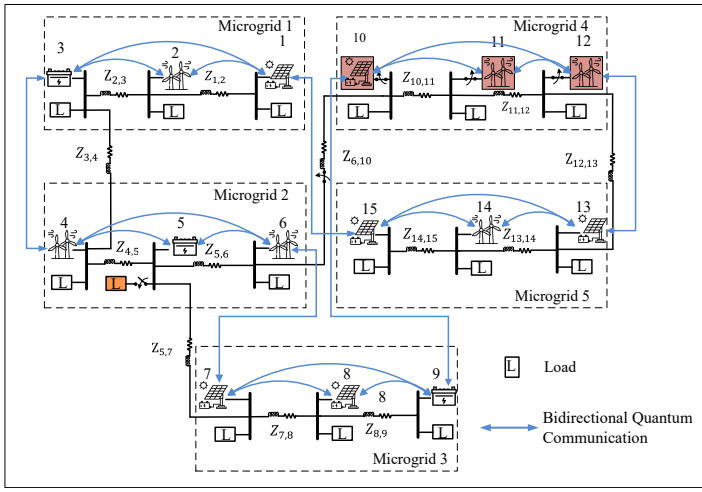

Parameter	Value	Parameter	Value
n_1, n_{13}	4×10^{-3}	n_2, n_{14}	4.5×10^{-3}
n_3, n_{15}	5×10^{-3}	n_4, n_7	10^{-3}
n_5, n_8	1.5×10^{-3}	n_6, n_9	2×10^{-3}
n_{10}	2.5×10^{-3}	n_{11}	3×10^{-3}
n_{12}	3.5×10^{-3}	Nominal frequency	60Hz
Nominal Voltage	380	Filter Capacitance	16μf
Filter Inductance	1.5mH	Output Impedance	1.5mH
$Z_{1,2}$, $Z_{4,5}$, $Z_{7,8}$, $Z_{10,11}$, $Z_{13,14}$	0.65Ω, 1.3mH	$Z_{2,3}$, $Z_{5,6}$, $Z_{8,9}$, $Z_{11,12}$, $Z_{14,15}$	0.5Ω, 1mH
$Z_{1,4}$, $Z_{5,7}$	0.35Ω, 1.8mH	$Z_{6,10}$	0.8Ω, 4mH
$Z_{12,13}$	0.7Ω, 2mH		

Fig. 6. Networked AC microgrids diagram and parameters - Blue bidirectional arrows represent the undirected quantum communications - To show the controller performance, the highlighted load at Microgrid 2 is attached and detached - At the case of plug-and-play of DERs, the highlighted DER_{10}, DER_{11} and DER_{12} in Microgrid 4 are disconnected and reconnected again.

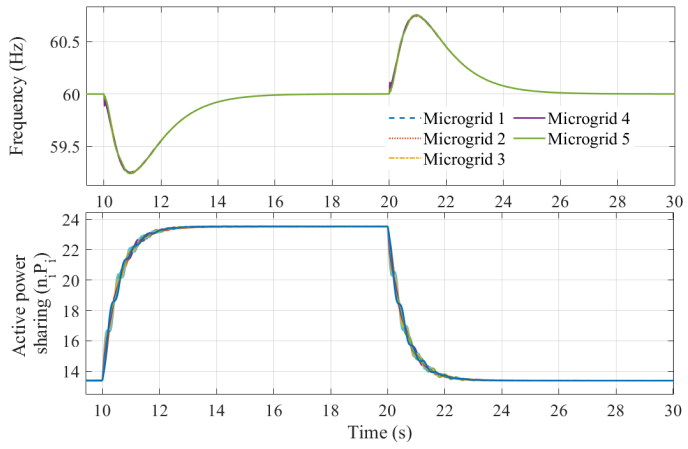

Fig. 7. DERs' frequencies throughout the network after attaching and detaching the step load.

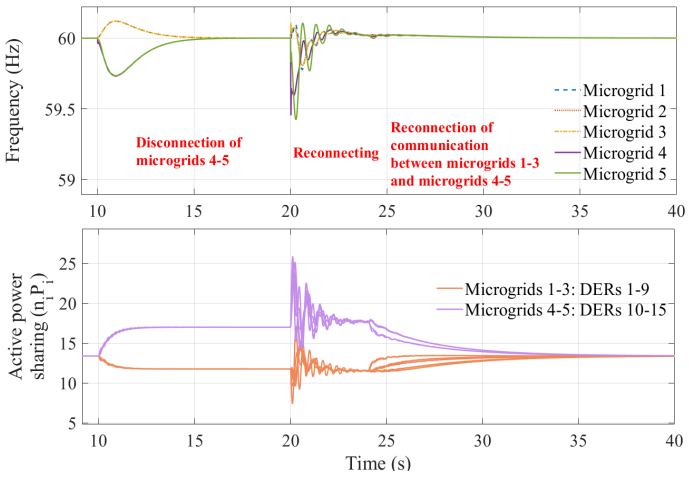

Fig. 9. Frequency regulation and active power sharing after plug-and-play of microgrids 4-5.

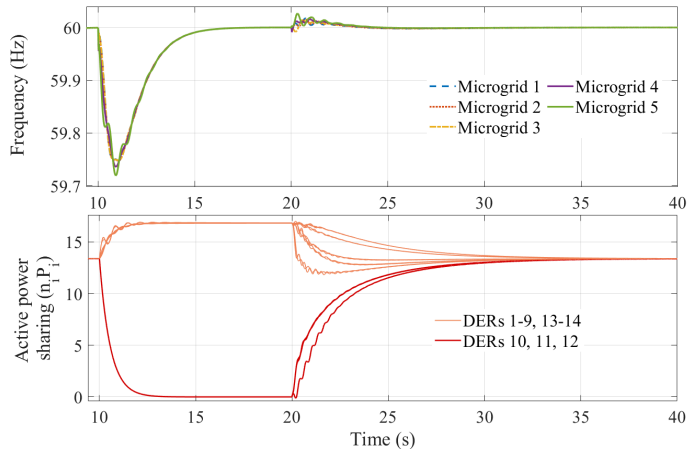

Fig. 8. Frequency regulation and active power sharing after plug-and-play of DERs 10, 11 and 12.

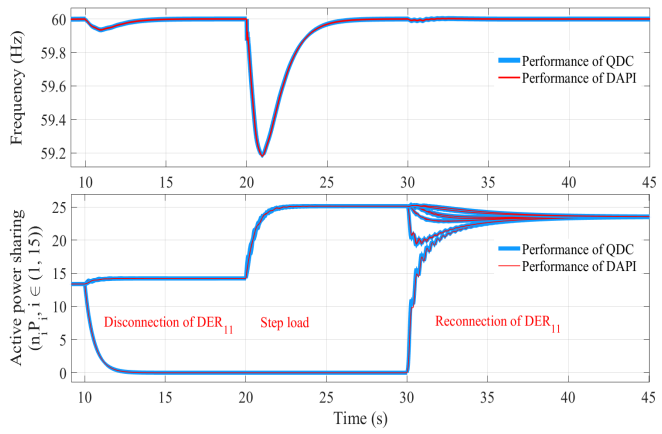

Fig. 10. Comparison between QDC and DAPI at the face of step load and plug-and-play events.

QDC's feature of plug-and-play capability. This merit is investigated, by detaching DER_{10}, DER_{11} and DER_{12} at t = 10s and plugging them in again at t = 20s. As depicted in Fig. 8, after disconnection of the DERs, the power deficiency reallocated among the remaining DERs and they manage to share the loads. As shown, accurate active power sharing and frequency restoration are maintained during plug-and-play operation.

3) Plug-and-play of microgrids: As the second plug-and-play scenario, microgrids 4 and 5 are disconnected from microgrids 1, 2 and 3 at t = 10s and reconnected again at t = 20s. Afterward, at t = 24s, the communication between microgrids 1-5 and microgrids 3-4 are reestablished. Fig. 9 shows how after disconnection of microgrids frequency is regulated in both microgrids 1-3 and 4-5 to the rated 60 Hz. Furthermore, after disconnection, the active power is shared among DERs 1-9 and DERs 10-15, and then among all the DERs after reconnection of microgrids 4-5, starting from t=24s. The reason of transient oscillations after reconnection is that, no presynchronization is implemented ahead of reconnection.

4) Comparison with the classical benchmark: In order to benchmark the QDC better, its performance is compared with the distributed-averaging PI (DAPI) controller (with the positive constant $k_i = 1$ [62]). For both DAPI and QDC, the communication graph is the same as Fig. 6. In this case, DER_{11} is unplugged at t = 10s followed by the step load of 40 kw at t = 20s, and then reconnected at t = 30s. Results depicted in Fig. 10 demonstrate that, regarding restoring time at the events of load disturbance and plug-and-play, both controllers have close performances. However, our devised QDC enables encoding information into quantum states, directly sent over quantum channels among participating DERs, and thus allows microgrids to be profited from quantum communication advantages.

C. Quantum Distributed Voltage Control for DC Microgrids.

In DC microgrids, droop control function is mainly utilized to provide decentralized power sharing. It generates the voltage reference V_i^{ref} as [63]

$$V_i^{\text{ref}} = V^* - d_i I_i \tag{28}$$

where V^* is the nominal dc voltage, d_i is the current droop gain, I_i is the output current of DER_i. Consider the DC microgrid depicted in Fig. (11), ignoring the inductance effect of lines, the DC bus voltage V_b can be determined as

$$V_b = V_i^{\text{ref}} - R_i I_i \tag{29}$$

It can be easily shown that, if the current droop gain d_i is set much larger than the line resistance R_i, $\frac{I_i}{I_j} \approx \frac{d_i}{d_j}$ and $V_b \approx V_i^{ref}$ $\forall i, j$. The larger d_i is chosen, the more accurate power sharing can be obtained, however, larger d_i may cause the dc bus voltage V_b to deviate more from the nominal value V^*. Therefore, we aim to attain both power sharing and precise voltage restoration, simultaneously, by adding the QDC. To equip the DC microgrid with the QDC, we follow the same implementation procedure explained for distributed frequency control and hence, the droop function (28) is modified as

$$\begin{aligned} V_i^{ref} &= V^* - d_i I_i + \frac{\phi_i}{c}, \\ \dot{\phi}_i &= \sin\left(c d_i I_i - \phi_i\right) + \sum_{j=1}^{n} a_{i,j} \sin\left(\phi_j - \phi_i\right), \end{aligned} \tag{30}$$

which can be rewritten as

$$\begin{aligned} V_i^{\text{ref}} &= V^* - m_i P_{dc,i} + \frac{\phi_i}{c}, \\ \dot{\phi}_i &= \sin\left(c m_i P_{dc,i} - \phi_i\right) + \sum_{j=1}^{n} a_{i,j} \sin\left(\phi_j - \phi_i\right), \end{aligned} \tag{31}$$

where $P_{dc,i} = V_b I_i$ and m_i is the power droop gain. Again, we select c such that $c < \frac{\pi/2}{\max(m_i P_{dc,i})}$, so that, it is ready to be incorporated into the argument of the rotation-Z operator at node i and then the process follows the steps explained in Fig. (3). As can be seen, (31) has a similar form as (26). Obviously, the first part in (31) is to drive the dc bus voltage V_b to the nominal value V^* while the second part is to guarantee that $\phi_i = \phi_j$ is satisfied, i.e., the current/power sharing is achieved which demonstrates that the QDC is also applicable to distributed voltage control in DC microgrids.

D. Verification on a DC Microgrid Case Study.

This case verifies the universality of the QDC. This merit is investigated by equipping a 9 DER DC microgrid case study with the QDC (see Fig. 11) and applying a step load of 267 kw at t= 10s. Results are depicted in Fig. 12. The exploited communication graph is shown in Fig. 12. As can be seen, voltage regulation is guaranteed throughout the step load disturbance and power/current is accurately shared among the heterogeneous DGs throughout the entire runtime.

V. Discussion, Conclusion and Outlook

A. Realization.

In an abstract sense, a quantum network is a network of quantum processors as nodes on specific locations, that are connected via links [64]. Like a quantum network/internet, realization of the QDC requires essential quantum hardware/software elements. First, a physical link (quantum channel) that is able to transmit qubits is needed. Standard telecom fibers are of suitable choices since they are currently used to communicate classical light and so far, photons are known as the ideal physical carrier of information to implement intrinsically secure quantum communications, specifically, for long-distance communications [10]. Various required building blocks for the links such as photonic quantum channels between ground stations or, between ground stations and satellites, quantum repeaters, quantum memory, etc., have recently been experimentally demonstrated [65], [66].

Second, a quantum algorithm is required to simulate Eq. (14) at each node. Several methods have been recently proposed for the problem of simulating open quantum systems represented by either the operator sum representation or the Lindblad master equation [67]–[69]. The overall approach in these algorithms is first, transforming the open dynamic into Kraus formalism in the operator sum form (if it is in Lindblad representation), which is the most general form of the time evolution for a density matrix, second, converting the Kraus operators into unitary matrices and third, decomposing the unitary matrices into unitary quantum gates. This procedure allows the evolution of the initial state through unitary quantum gates.

The third element is measurement. In a typical quantum algorithm, we need to estimate expectation values of a set of

This article has been accepted for publication in IEEE Transactions on Power Systems. This is the author's version which has not been fully edited and content may change prior to final publication. Citation information: DOI 10.1109/TPWRS.2022.3196608

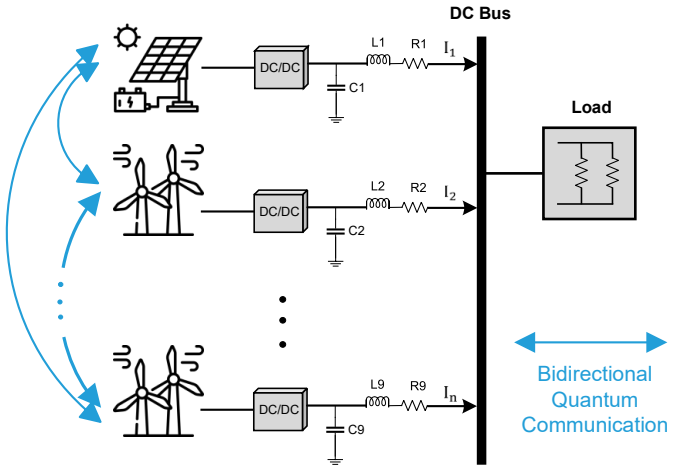

Parameter	Value
DC-Link Voltage	200 V
Filter Inductance	$L_1, L_2, L_5, L_6, L_7, L_9 = 5e^{-3}$ $L_3 = 4e^{-3}$ $L_4 = 4.5e^{-3}$ $L_8 = 5.5e^{-3}$
Filter Capacitance	$C_1, C_4, C_6, C_9 = 20e^{-6}$ $C_2, C_5, C_7 = 30e^{-6}$ $C_3, C_8 = 40e^{-6}$
Line Resistance	$R_1, R_3, R_7, R_9 = 0.02\ \Omega$ $R_4, R_6 = 0.015\Omega$, $R_5, R_8 = 0.025\ \Omega$ $R_2 = 0.01\ \Omega$
Droop Gain	$m_1 = 5e^{-3}$, $m_2 = 4e^{-3}$, $m_3 = 3e^{-3}$, $m_4 = 2e^{-3}$, $m_5 = 1e^{-3}$, $m_6 = 6e^{-3}$, $m_7 = 7e^{-3}$, $m_8 = 8e^{-3}$, $m_9 = 9e^{-3}$
Voltage Loop	$K_{VP} = 0.12$, $K_{VI} = 6$
Current Loop	$K_{IP} = 0.2$, $K_{II} = 1e^{-4}$
Load	$R_L = 0.15\ \Omega$

Fig. 11. DC microgrid model quipped with the QDC and parameters.

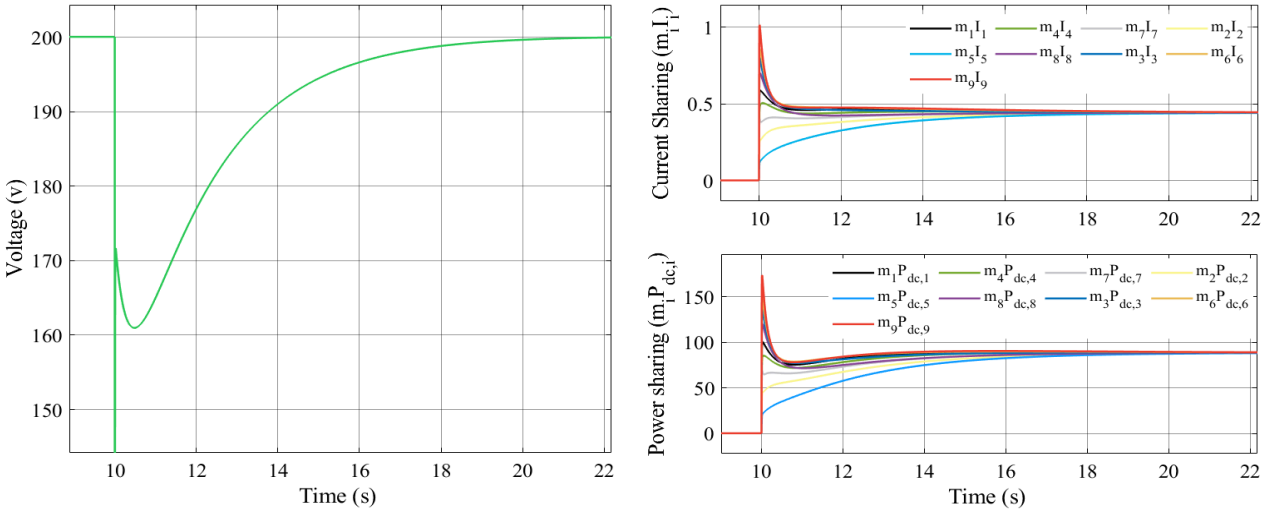

Fig. 12. Voltage regulation, power sharing and current sharing after a step load disturbance at t=10s.

operators/observables in a quantum state ρ that can be prepared repeatedly using a programmable quantum system [70]. As discussed, each $\phi_i(t)$ is the averaged measurement outcome which is obtained by averaging measurement outcomes of many realizations of a single experiment for node i. The reason is, an informative quantum measurement is demolishing (i.e. causing the wave function to collapse) and gives probabilistic outcomes [71]. Hence, to obtain precise estimates, each operator must be measured many times.

Several solutions have been introduced to overcome this fundamental scaling problem including matrix product state tomography, neural network tomography, shadow tomography and classical shadow [71]–[76]. Among these methods, the derandomized Pauli measurement approach in [70] is of our interest, where authors describe a deterministic protocol for estimating Pauli-operator expectation values using very few copies of ρ. Developments like these are of particular importance since they are proposing promising solutions to the issues of large shot counts and high number of times required for transmitting a particular quantum state among two nodes for measurement purposes.

B. Conclusion and Outlook.

While we are on the verge of quantum internet, planning for future smart power grids, as the largest man-made systems, based on classical communications seems obsolete and may fail to address the new requirements and security challenges. Therefore, keeping up with the quantum technology seems essential. The potential to design a quantum synchronization scheme motivated us to study the feasibility of realizing a quantum distributed controller.

In this work we introduce a new synchronization mechanism by leveraging the quantum properties of qubits. Since the distributed control problems of microgrids can be modeled as networked differential equations, we leverage a proposed master equation to construct the network of differential equations. Then, we demonstrate that by characterizing proper observables, expectation values of all the observers at all nodes will eventu-

ally get synchronized to a possibly time-varying target value and the synchronization rule follows the forced Kuramoto model. We show how our proposed quantum synchronization scheme can be exploited to regulate AC microgrids' frequency and DC microgrids' voltage and guarantee precise power sharing. Then, our theoretical derivations are complemented by a series of numerical and simulation results, which have fully confirm the validity and generality of the QDC scheme. In later studies, we will demonstrate that, due to the superposition feature of qubits, the QDC provides a foundation for introducing more enhanced quantum-secure distributed control for microgrids through randomizing the θ angle of qubits in the initialization step, which finally results in an unprecedented security for distributed control of AC and DC microgrids.

Although, in our devised protocol, communication network is assumed balanced, we believe the QDC can be extended to unbalanced communications where the Laplacian matrix is no longer doubly stochastic. Further, the QDC in conjunction with sparse data transmission and event-triggered methods, promises wide adoptions in those applications where resilient high-speed communication is required and computation burden matters.

ACKNOWLEDGEMENT

We would like to thank the Brookhaven National Laboratory operated IBM-Q Hub. This research also used resources of the Oak Ridge Leadership Computing Facility, which is a DOE Office of Science User Facility supported under Contract DE-AC05-00OR22725.

REFERENCES

[1] P. Zhang, *Networked Microgrids*. Cambridge, U.K.: Cambridge University Press, 2021.

[2] F. Feng and P. Zhang, "Enhanced microgrid power flow incorporating hierarchical control," *IEEE Transactions on Power Systems*, vol. 35, no. 3, pp. 2463–2466, 2020.

[3] T. Morstyn, N. Farrell, S. J. Darby, and M. D. McCulloch, "Using peer-to-peer energy-trading platforms to incentivize prosumers to form federated power plants," *Nature Energy*, vol. 3, no. 2, pp. 94–101, 2018.

[4] F. Molnar, T. Nishikawa, and A. E. Motter, "Asymmetry underlies stability in power grids," *Nature communications*, vol. 12, no. 1, pp. 1–9, 2021.

[5] P. J. Menck, J. Heitzig, J. Kurths, and H. J. Schellnhuber, "How dead ends undermine power grid stability," *Nature communications*, vol. 5, no. 1, pp. 1–8, 2014.

[6] P. Babahajiani, Q. Shafiee, and H. Bevrani, "Intelligent demand response contribution in frequency control of multi-area power systems," *IEEE Transactions on Smart Grid*, vol. 9, no. 2, pp. 1282–1291, 2018.

[7] H. Bevrani, P. R. Daneshmand, P. Babahajyani, Y. Mitani, and T. Hiyama, "Intelligent lfc concerning high penetration of wind power: Synthesis and real-time application," *IEEE Transactions on Sustainable Energy*, vol. 5, no. 2, pp. 655–662, 2014.

[8] P. Babahajiani, L. Wang, J. Liu, and P. Zhang, "Push-sum-enabled resilient microgrid control," *IEEE Transactions on Smart Grid*, vol. 12, no. 4, pp. 3661–3664, 2021.

[9] G. Lou, W. Gu, X. Lu, Y. Xu, and H. Hong, "Distributed secondary voltage control in islanded microgrids with consideration of communication network and time delays," *IEEE Transactions on Smart Grid*, vol. 11, no. 5, pp. 3702–3715, 2020.

[10] S. Wehner, D. Elkouss, and R. Hanson, "Quantum internet: A vision for the road ahead," *Science*, vol. 362, no. 6412, 2018.

[11] S. Sahoo, T. Dragičević, and F. Blaabjerg, "Multilayer resilience paradigm against cyber attacks in dc microgrids," *IEEE Trans. Power Electron.*, vol. 36, no. 3, pp. 2522–2532, 2021.

[12] M. S. Sadabadi, S. Sahoo, and F. Blaabjerg, "A fully resilient cyber-secure synchronization strategy for ac microgrids," *IEEE Trans. Power Electron.*, vol. 36, no. 12, pp. 13 372–13 378, 2021.

[13] Y. Chen, D. Qi, H. Dong, C. Li, Z. Li, and J. Zhang, "A fdi attack-resilient distributed secondary control strategy for islanded microgrids," *IEEE Trans. Smart Grid*, vol. 12, no. 3, pp. 1929–1938, 2021.

[14] S. Sahoo, Y. Yang, and F. Blaabjerg, "Resilient synchronization strategy for ac microgrids under cyber attacks," *IEEE Trans. Power Electron.*, vol. 36, no. 1, pp. 73–77, 2021.

[15] S. Zuo, O. A. Beg, F. L. Lewis, and A. Davoudi, "Resilient networked ac microgrids under unbounded cyber attacks," *IEEE trans. Smart Grid*, vol. 11, no. 5, pp. 3785–3794, 2020.

[16] A. Bidram, B. Poudel, L. Damodaran, R. Fierro, and J. M. Guerrero, "Resilient and cybersecure distributed control of inverter-based islanded microgrids," *IEEE Trans. Ind. Informat.*, vol. 16, no. 6, pp. 3881–3894, 2020.

[17] S. Zuo, T. Altun, F. L. Lewis, and A. Davoudi, "Distributed resilient secondary control of dc microgrids against unbounded attacks," *IEEE trans. Smart Grid*, vol. 11, no. 5, pp. 3850–3859, 2020.

[18] G. Fano and S. Blinder, "Chapter 11 - quantum chemistry on a quantum computer," in *Mathematical Physics in Theoretical Chemistry*, ser. Developments in Physical & Theoretical Chemistry, S. Blinder and J. House, Eds. Elsevier, 2019, pp. 377 – 400.

[19] K. Wright, K. Beck, S. Debnath, J. Amini, Y. Nam, N. Grzesiak, J.-S. Chen, N. Pisenti, M. Chmielewski, C. Collins *et al.*, "Benchmarking an 11-qubit quantum computer," *Nature communications*, vol. 10, no. 1, pp. 1–6, 2019.

[20] R. Qi, Z. Sun, Z. Lin, P. Niu, W. Hao, L. Song, Q. Huang, J. Gao, L. Yin, and G.-L. Long, "Implementation and security analysis of practical quantum secure direct communication," *Light: Science & Applications*, vol. 8, no. 1, pp. 1–8, 2019.

[21] G. Popkin, "The internet goes quantum," *Science*, vol. 372, no. 6546, pp. 1026–1029, 2021.

[22] H. J. Kimble, "The quantum internet," *Nature*, vol. 453, no. 7198, pp. 1023–1030, 2008.

[23] Y. Yu, F. Ma, X.-Y. Luo, B. Jing, P.-F. Sun, R.-Z. Fang, C.-W. Yang, H. Liu, M.-Y. Zheng, X.-P. Xie *et al.*, "Entanglement of two quantum memories via fibres over dozens of kilometres," *Nature*, vol. 578, no. 7794, pp. 240–245, 2020.

[24] D. Castelvecchi, "Quantum network is step towards ultrasecure internet," *Nature*, vol. 590, no. 7847, pp. 540–541, 2021.

[25] K. Azuma, A. Mizutani, and H.-K. Lo, "Fundamental rate-loss trade-off for the quantum internet," *Nature communications*, vol. 7, no. 1, pp. 1–8, 2016.

[26] S. Pirandola and S. L. Braunstein, "Physics: Unite to build a quantum internet," *Nature News*, vol. 532, no. 7598, p. 169, 2016.

[27] D. Castelvecchi, "The quantum internet has arrived (and it hasn't)." *Nature*, vol. 554, no. 7690, pp. 289–293, 2018.

[28] J. P. Dowling, *Schrödinger's Web: Race to Build the Quantum Internet*. CRC Press, 2020.

[29] Z. Jiang, Z. Tang, Y. Qin, C. Kang, and P. Zhang, "Quantum internet for resilient electric grids," *International Transactions on Electrical Energy Systems*, vol. 31, no. 6, p. e12911, 2021.

[30] B. K. Park, M. K. Woo, Y.-S. Kim, Y.-W. Cho, S. Moon, and S.-W. Han, "User-independent optical path length compensation scheme with sub-nanosecond timing resolution for a $1\times$ n quantum key distribution network system," *Photonics Research*, vol. 8, no. 3, pp. 296–302, 2020.

[31] Y.-H. Luo, H.-S. Zhong, M. Erhard, X.-L. Wang, L.-C. Peng, M. Krenn, X. Jiang, L. Li, N.-L. Liu, C.-Y. Lu *et al.*, "Quantum teleportation in high dimensions," *Physical review letters*, vol. 123, no. 7, p. 070505, 2019.

[32] Z. Qi, Y. Li, Y. Huang, J. Feng, Y. Zheng, and X. Chen, "A 15-user quantum secure direct communication network," *Light: Science & Applications*, vol. 10, no. 1, pp. 1–8, 2021.

[33] J.-Y. Hu, B. Yu, M.-Y. Jing, L.-T. Xiao, S.-T. Jia, G.-Q. Qin, and G.-L. Long, "Experimental quantum secure direct communication with single photons," *Light: Science & Applications*, vol. 5, no. 9, pp. e16 144–e16 144, 2016.

[34] S. Pirandola, S. Mancini, S. Lloyd, and S. L. Braunstein, "Continuous-variable quantum cryptography using two-way quantum communication," *Nature Physics*, vol. 4, no. 9, pp. 726–730, 2008.

[35] S. K. Joshi, D. Aktas, S. Wengerowsky, M. Lončarić, S. P. Neumann, B. Liu, T. Scheidl, G. C. Lorenzo, Ž. Samec, L. Kling *et al.*, "A trusted node–free eight-user metropolitan quantum communication network," *Science advances*, vol. 6, no. 36, p. eaba0959, 2020.

[36] S. Wengerowsky, S. K. Joshi, F. Steinlechner, H. Hübel, and R. Ursin, "An entanglement-based wavelength-multiplexed quantum communication network," *Nature*, vol. 564, no. 7735, pp. 225–228, 2018.

[37] Y.-A. Chen, Q. Zhang, T.-Y. Chen, W.-Q. Cai, S.-K. Liao, J. Zhang, K. Chen, J. Yin, J.-G. Ren, Z. Chen *et al.*, "An integrated space-to-ground quantum communication network over 4,600 kilometres," *Nature*, vol. 589, no. 7841, pp. 214–219, 2021.

[38] A. Jadbabaie, J. Lin, and A. Morse, "Coordination of groups of mobile autonomous agents using nearest neighbor rules," *IEEE Transactions on Automatic Control*, vol. 48, no. 6, pp. 988–1001, 2003.

[39] R. Olfati-Saber and R. M. Murray, "Consensus problems in networks of agents with switching topology and time-delays," *IEEE Transactions on Automatic Control*, vol. 49, no. 9, pp. 1520–1533, 2004.

[40] R. Sepulchre, A. Sarlette, and P. Rouchon, "Consensus in non-commutative spaces," in *49th IEEE Conference on Decision and Control (CDC)*, 2010, pp. 6596–6601.

[41] L. Mazzarella, A. Sarlette, and F. Ticozzi, "Consensus for quantum networks: Symmetry from gossip interactions," *IEEE Transactions on Automatic Control*, vol. 60, no. 1, pp. 158–172, 2015.

[42] L. Mazzarella, F. Ticozzi, and A. Sarlette, "Extending robustness and randomization from consensus to symmetrization algorithms," *SIAM Journal on Control and Optimization*, vol. 53, no. 4, pp. 2076–2099, 2015.

[43] H.-P. Breuer and F. Petruccione, *The Theory of Open Quantum Systems: 1st Edition*. Oxford Univ. Press, 2002.

[44] G. Lindblad, "On the generators of quantum dynamical semigroups," *Comm. Math. Phys.*, vol. 48, no. 2, pp. 119–130, 1976.

[45] G. Shi, D. Dong, I. R. Petersen, and K. H. Johansson, "Reaching a quantum consensus: Master equations that generate symmetrization and synchronization," *IEEE Transactions on Automatic Control*, vol. 61, no. 2, pp. 374–387, 2016.

[46] C. Godsil and G. Royle, *Algebraic Graph Theory*. Springer-Verlag, 2001.

[47] M. A. Nielsen and I. L. Chuang, *Quantum Computation and Quantum Information: 10th Anniversary Edition*. Cambridge University Press, 2010.

[48] J. Preskill, "Lecture notes for physics: Quantum information and computation," 1998.

[49] S. Lloyd, G. De Palma, C. Gokler, B. Kiani, Z.-W. Liu, M. Marvian, F. Tennie, and T. Palmer, "Quantum algorithm for nonlinear differential equations," *arXiv preprint arXiv:2011.06571*, 2020.

[50] A. M. Childs, J.-P. Liu, and A. Ostrander, "High-precision quantum algorithms for partial differential equations," *arXiv preprint arXiv:2002.07868*, 2020.

[51] I. Joseph, "Koopman–von neumann approach to quantum simulation of nonlinear classical dynamics," *Physical Review Research*, vol. 2, no. 4, p. 043102, 2020.

[52] D. W. Berry, A. M. Childs, A. Ostrander, and G. Wang, "Quantum algorithm for linear differential equations with exponentially improved dependence on precision," *Communications in Mathematical Physics*, vol. 356, no. 3, pp. 1057–1081, 2017.

[53] A. Engel, G. Smith, and S. E. Parker, "Quantum algorithm for the vlasov equation," *Physical Review A*, vol. 100, no. 6, p. 062315, 2019.

[54] P. C. Costa, S. Jordan, and A. Ostrander, "Quantum algorithm for simulating the wave equation," *Physical Review A*, vol. 99, no. 1, p. 012323, 2019.

[55] A. W. Harrow, A. Hassidim, and S. Lloyd, "Quantum algorithm for linear systems of equations," *Physical review letters*, vol. 103, no. 15, p. 150502, 2009.

[56] H. M. Wiseman and G. J. Milburn, *Quantum measurement and control*. Cambridge university press, 2009.

[57] E. Ott and T. M. Antonsen, "Low dimensional behavior of large systems of globally coupled oscillators," *Chaos: An Interdisciplinary Journal of Nonlinear Science*, vol. 18, no. 3, p. 037113, 2008.

[58] J. Johansson, P. Nation, and F. Nori, "Qutip 2: A python framework for the dynamics of open quantum systems," *Computer Physics Communications*, vol. 184, no. 4, pp. 1234 – 1240, 2013.

[59] X. Lu, X. Yu, J. Lai, Y. Wang, and J. M. Guerrero, "A novel distributed secondary coordination control approach for islanded microgrids," *IEEE Trans. on Smart Grid*, vol. 9, no. 4, pp. 2726–2740, July 2018.

[60] N. Pogaku, M. Prodanovic, and T. C. Green, "Modeling, analysis and testing of autonomous operation of an inverter-based microgrid," *IEEE Transactions on Power Electronics*, vol. 22, no. 2, pp. 613–625, 2007.

[61] M. Shi, X. Chen, M. Shahidehpour, Q. Zhou, and J. Wen, "Observer-based resilient integrated distributed control against cyberattacks on sensors and actuators in islanded ac microgrids," *IEEE Transactions on Smart Grid*, vol. 12, no. 3, pp. 1953–1963, 2021.

[62] J. W. Simpson-Porco, Q. Shafiee, F. Dörfler, J. C. Vasquez, J. M. Guerrero, and F. Bullo, "Secondary frequency and voltage control of islanded microgrids via distributed averaging," *IEEE Transactions on Industrial Electronics*, vol. 62, no. 11, pp. 7025–7038, 2015.

[63] V. Nasirian, A. Davoudi, F. L. Lewis, and J. M. Guerrero, "Distributed adaptive droop control for dc distribution systems," *IEEE Transactions on Energy Conversion*, vol. 29, no. 4, pp. 944–956, 2014.

[64] K. Hansenne, Z.-P. Xu, T. Kraft, and O. Gühne, "Symmetries in quantum networks lead to no-go theorems for entanglement distribution and to verification techniques," *Nature Communications*, vol. 13, no. 1, pp. 1–6, 2022.

[65] J. Yin, Y.-H. Li, S.-K. Liao, M. Yang, Y. Cao, L. Zhang, J.-G. Ren, W.-Q. Cai, W.-Y. Liu, S.-L. Li *et al.*, "Entanglement-based secure quantum cryptography over 1,120 kilometres," *Nature*, vol. 582, no. 7813, pp. 501–505, 2020.

[66] S.-K. Liao, W.-Q. Cai, J. Handsteiner, B. Liu, J. Yin, L. Zhang, D. Rauch, M. Fink, J.-G. Ren, W.-Y. Liu *et al.*, "Satellite-relayed intercontinental quantum network," *Physical review letters*, vol. 120, no. 3, p. 030501, 2018.

[67] Z. Hu, R. Xia, and S. Kais, "A quantum algorithm for evolving open quantum dynamics on quantum computing devices," *Scientific reports*, vol. 10, no. 1, pp. 1–9, 2020.

[68] K. Head-Marsden, S. Krastanov, D. A. Mazziotti, and P. Narang, "Capturing non-markovian dynamics on near-term quantum computers," *Physical Review Research*, vol. 3, no. 1, p. 013182, 2021.

[69] A. W. Schlimgen, K. Head-Marsden, L. M. Sager, P. Narang, and D. A. Mazziotti, "Quantum simulation of open quantum systems using a unitary decomposition of operators," *Physical Review Letters*, vol. 127, no. 27, p. 270503, 2021.

[70] H.-Y. Huang, R. Kueng, and J. Preskill, "Efficient estimation of pauli observables by derandomization," *Physical Review Letters*, vol. 127, no. 3, p. 030503, 2021.

[71] ——, "Predicting many properties of a quantum system from very few measurements," *Nature Physics*, vol. 16, no. 10, pp. 1050–1057, 2020.

[72] H.-Y. Huang, "Learning quantum states from their classical shadows," *Nature Reviews Physics*, pp. 1–1, 2022.

[73] M. Cramer, M. B. Plenio, S. T. Flammia, R. Somma, D. Gross, S. D. Bartlett, O. Landon-Cardinal, D. Poulin, and Y.-K. Liu, "Efficient quantum state tomography," *Nature communications*, vol. 1, no. 1, pp. 1–7, 2010.

[74] J. Carrasquilla, G. Torlai, R. G. Melko, and L. Aolita, "Reconstructing quantum states with generative models," *Nature Machine Intelligence*, vol. 1, no. 3, pp. 155–161, 2019.

[75] G. Torlai, G. Mazzola, J. Carrasquilla, M. Troyer, R. Melko, and G. Carleo, "Neural-network quantum state tomography," *Nature Physics*, vol. 14, no. 5, pp. 447–450, 2018.

[76] S. Aaronson and G. N. Rothblum, "Gentle measurement of quantum states and differential privacy," in *Proceedings of the 51st Annual ACM SIGACT Symposium on Theory of Computing*, 2019, pp. 322–333.

Pouya Babahajiani (Senior Member, IEEE) received the B.S. degree in electrical engineering from University of Kurdistan, Sanandaj, Iran, in 2009, and the M.Sc. degree in control engineering from Isfahan University of Technology, Isfahan, Iran, in 2012. He is currently pursuing his Ph.D. degree in electrical and computer engineering at Stony Brook University, NY, USA. His research interests include quantum computing, distributed control, and microgrid stability and control.

Peng Zhang (Senior Member, IEEE) received the Ph.D. degree in electrical engineering from the University of British Columbia, Vancouver, BC, Canada, in 2009. He is a Full Professor of Electrical and Computer Engineering, and a SUNY Empire Innovation Professor at Stony Brook University, New York. He has a joint appointment at Brookhaven National Laboratory as a Staff Scientist. Previously, he was a Centennial Associate Professor and a Francis L. Castleman Associate Professor at the University of Connecticut, Storrs, CT, USA. He was a System Planning Engineer at BC Hydro and Power Authority, Canada, during 2006-2010. His research interests include AI-enabled smart grids, quantum-engineered power grids, networked microgrids, power system stability and control, cybersecurity, and formal methods and reachability analysis.

Dr. Zhang is an individual member of CIGRÉ. He is an Editor for the IEEE Transactions on Power Systems, the IEEE Power and Energy Society Letters, and the IEEE Journal of Oceanic Engineering.

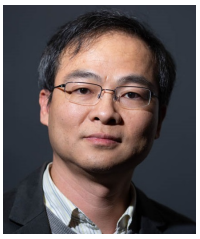

Tzu-Chieh Wei received his PhD in Physics from the University of Illinois at Urbana-Champaign in 2004 and stayed there as a postdoctoral associate until 2007. He then worked as a postdoctoral fellow at the Institute for Quantum Computing, at University of Waterloo, and focused on quantum information processing and quantum computational complexity. Later in 2009, he moved to the University of British Columbia and studied various models of quantum computation, and in particular, connected the one-way quantum computer to condensed matter physics. In 2011, he joined the faculty of the C.N. Yang Institute for Theoretical Physics and Department of Physics and Astronomy at Stony Brook University, where he is currently an Associate Professor. His current interests include quantum information and computation, topological phases, and numerical simulations of quantum systems using various tensor-network methods.

Ji Liu (Member, IEEE) received the B.S. degree in information engineering from Shanghai Jiao Tong University, Shanghai, China, in 2006, and the Ph.D. degree in electrical engineering from Yale University, New Haven, CT, USA, in 2013. He is currently an Assistant Professor in the Department of Electrical and Computer Engineering at Stony Brook University, Stony Brook, NY, USA. Prior to that, he was a Postdoctoral Research Associate at the Coordinated Science Laboratory, University of Illinois at Urbana-Champaign, Urbana, IL, USA, and the School of Electrical, Computer and Energy Engineering, Arizona State University, Tempe, AZ, USA. He is an Associate Editor of the IEEE Transactions on Signal and Information Processing over Networks. His current research interests include distributed control and optimization, distributed machine learning, distributed quantum computing, epidemic networks, social networks, and cyber-physical systems.

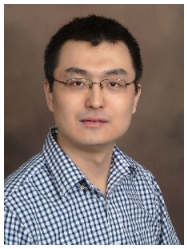

Xiaonan Lu (Member, IEEE) received his B.E. and Ph.D. degrees in electrical engineering from Tsinghua University, Beijing, China, in 2008 and 2013, respectively. From September 2010 to August 2011, he was a guest Ph.D. student at the Department of Energy Technology, Aalborg University, Denmark. From October 2013 to December 2014, he was a Postdoc Research Associate at the Department of Electrical Engineering and Computer Science, University of Tennessee, Knoxville. From January 2015 to July 2018, he was with the Energy Systems Division, Argonne National Laboratory, first as a Postdoc Appointee and then as an Energy Systems Scientist. From July 2018 to July 2022, he was with the College of Engineering at Temple University as an Assistant Professor. In August 2022, he joined the School of Engineering Technology at Purdue University as an Associate Professor. His research interests include modeling, control and design of power electronic inverters, hybrid AC and DC microgrids, and real-time hardware-in-the-loop simulation. Dr. Lu is the Associate Editor of IEEE Transactions on Industrial Electronics, the Associate Editor of IEEE Transactions on Industry Applications, the Editor of IEEE Transactions on Smart Grid, and the Editor of Power Engineering Letters. He serves as the Chair of the Industrial Power Converters Committee (IPCC) in the IEEE Industry Applications Society (IAS). He is also the recipient of the 2020 Young Engineer of the Year Award in the IEEE Philadelphia Section.